

# Continuous hollow $\alpha$ -Fe<sub>2</sub>O<sub>3</sub> and $\alpha$ -Fe fibers prepared by the sol-gel method

Cairong Gong, Dairong Chen,\* Xiuling Jiao and Qilong Wang

Department of chemistry, Shandong University, Jinan 250100, P. R. China.  
E-mail: cdr@sdu.edu.cn

Received 4th February 2002, Accepted 8th April 2002

First published as an Advance Article on the web 26th April 2002

Continuous iron oxide gel fibers were prepared by the sol-gel method using ferric alkoxide and acetic acid as starting materials and alcohol as solvent, and continuous hollow  $\alpha$ -Fe<sub>2</sub>O<sub>3</sub> fibers produced after the gel fibers were heat treated at 400 °C for 1 h. The outer diameter of the  $\alpha$ -Fe<sub>2</sub>O<sub>3</sub> fibers is between 4–10  $\mu$ m and the wall thickness is 1–2  $\mu$ m, in which the  $\alpha$ -Fe<sub>2</sub>O<sub>3</sub> particle size is about 100 nm. 2-Methoxyethanol and acetic acid played important roles in the formation of the spinnable sol and the possible mechanism for the formation of the hollow  $\alpha$ -Fe<sub>2</sub>O<sub>3</sub> fibers was discussed in detail. The hollow  $\alpha$ -Fe fibers could be obtained by reducing the as-prepared  $\alpha$ -Fe<sub>2</sub>O<sub>3</sub> fibers under hydrogen flow and the  $\alpha$ -Fe particle size increased to  $\sim$ 150 nm.

## 1 Introduction

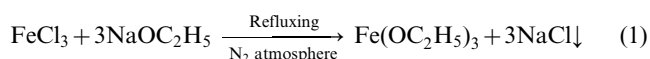
Tubular materials have attracted considerable attention because of their peculiar physico-chemical properties and potential applications in nanofabrication.<sup>1</sup> To date, several preparative approaches have been reported for the preparation of oxide tubes by the sol-gel method. Kozuka *et al.* prepared hollow YBa<sub>2</sub>Cu<sub>3</sub>O<sub>7-x</sub><sup>2</sup> and Bi-Pb-Sr-Ca-Cu-O<sup>3</sup> superconducting fibers composed of plate-like crystals as large as 5–10  $\mu$ m wide and 0.5  $\mu$ m thick using acetates as precursors. Aizawa *et al.*<sup>4</sup> synthesized hollow TiO<sub>2</sub> fibers from titanium tetraisopropoxide, in which the hollow part was typically 2 mm in length and occupied half of the total length of the fiber, and Kobayashi *et al.*<sup>5</sup> synthesized hollow TiO<sub>2</sub> fibers using supramolecular assemblies. Nakamura *et al.*<sup>6</sup> obtained a new type of silica-gel tube by a sol-gel method at room temperature and the products had square shapes with an outer diameter of 0.8–1.0  $\mu$ m and 200–300  $\mu$ m in length. Ono *et al.*<sup>7</sup> reported the synthesis of hollow silica nanofibers using different amphiphilic molecules as templates. However, the hollow fibers with short length would impose limitations on their potential applications. To the best of our knowledge, there have been no papers reported on the preparation of hollow  $\alpha$ -Fe<sub>2</sub>O<sub>3</sub> fibers. In this paper, continuous iron oxide green fibers were prepared from ferric alkoxide sol precursor, then the hollow hematite fibers were obtained after burning out the organic moieties from the green fibers. The length of the as-prepared fibers was as long as 20 cm and the outer diameter was between 4–20  $\mu$ m. Hematite is widely applied in catalysis<sup>8</sup> and gas sensing<sup>9</sup> and the as-prepared micro-tubes have potential applications in capillary electrophoresis. Furthermore, reduction of hematite in hydrogen atmosphere resulted in the formation of hollow  $\alpha$ -Fe fibers. As absorbing materials,  $\alpha$ -Fe fibers with large absorbing capacity in a wide frequency range are extensively applied in obscuring aircraft.<sup>10</sup> It is proposed that the hollow fibers might be applied as micro-reactors in catalytic reactions, which exhibit enhanced catalytic activity and facility compared with the corresponding bulk counterparts.<sup>11</sup> Furthermore, micro-nano devices can also be fabricated using the hollow fibers as host and nano-materials as guest.

## 2 Experimental

### 2.1 Synthesis

Iron(III) chloride was purchased from Shanghai Chemical Co. (P. R. China), absolute ethanol, benzene, 2-methoxyethanol and acetic acid were purchased from Tianjin Chemical Co. (P. R. China). All reagents were of analytical grade and further dehydrated before utilization.

Fe(OC<sub>2</sub>H<sub>5</sub>)<sub>3</sub> used as precursor was prepared in absolute ethanol according to eqn. (1):<sup>12</sup>



The sodium chloride was removed by centrifugation and the solution was distilled under reduced pressure and the remainder was then further purified by extraction with benzene, the product was kept in absolute ethanol to prevent Fe(OC<sub>2</sub>H<sub>5</sub>)<sub>3</sub> from hydrolyzing. 30 ml Fe(OC<sub>2</sub>H<sub>5</sub>)<sub>3</sub>/C<sub>2</sub>H<sub>5</sub>OH solution with concentration ranging from 0.45–0.96 mol dm<sup>-3</sup> was added into a three-necked flask containing some 2-methoxyethanol (MOE), the molar ratio (*n*) of iron(III) to MOE being 1 : 3. After refluxing for 2 h, a red deposit appeared in the solution, which was proved to be oligomeric ferric alkoxides by FT-IR spectroscopic investigation. Then acetic acid was added into the above system with the molar ratio of iron(III) to acetic acid being 1 : 10, the deposit dissolved and a clear solution was obtained. The solution was refluxed for an additional 2 h to give the precursor sol. The sol was transferred into a 100 ml beaker and conditioned at room temperature for 7 days and then kept at 40 °C for several days until gel fibers could be drawn from it. The aging time changed with the ferric alkoxide and the value of *n*. Table 1 gives the experimental conditions for preparing the spinnable sol. The gel fibers drawn from the spinnable sol were dried at room temperature for 2 days to remove free organic solvent, during which time the gelation continued. Subsequently, they were held at 200 °C for 2 h with the aim of removing the residual free organic compounds. Then they were further heated to 400 °C for 1 h to let the acetates decompose. Finally, the products were held at either 500, 600 or 750 °C for 1 h. The whole calcination process

**Table 1** Description of preparative condition of the spinnable sol

Sample	C/mol dm <sup>-3</sup>	V <sub>MOE</sub> /ml	V <sub>HAc</sub> /ml	Aging time/day
1	0.45	3.2	7.7	9
2	0.64	4.5	11	9
3	0.72	5.1	12.4	10
4	0.72	10.2	12.4	12
5	0.72	15.3	12.4	14
6	0.96	6.8	16.5	12

was carried out in air and the heating rate was 100 °C h<sup>-1</sup>. The as-prepared hollow hematite fibers were reduced in a tubular furnace under hydrogen flow at temperatures ranging between 340–380 °C for 0.5 h or 1 h;  $\alpha$ -Fe hollow fibers were prepared when the reacting time was 1 h.

The ferric acetate was prepared as follows: 13.3 g FeCl<sub>3</sub>·6H<sub>2</sub>O was dissolved in 50 ml of distilled water, and 5 ml aqueous ammonia (25%) was added dropwise. Then fresh ferric hydroxide was obtained by filtration and washed with distilled water several times. The product was dissolved in 200 ml of acetic acid with stirring for 4 h. After evaporation at 60 °C by water bath, the expected products were obtained.

## 2.2 Characterization

The phase of the fibers was identified by X-ray diffraction (XRD Rigaku D/Max 2200PC diffractometer with Cu-K $\alpha$  radiation and graphite monochromator) with a scanning rate of 8° min<sup>-1</sup> in the 2 $\theta$  range from 20 to 70°. Microscopic observation of the fibers was performed by scanning electron microscopy (SEM, Hitachi, Model S-520) under an accelerating voltage of 20 kV and by transmission electron microscopy (TEM, JEM-100CX) at an accelerating voltage of 100 kV. The infrared (IR) spectra of the products were measured using the KBr disc technique in the range 400–4000 cm<sup>-1</sup>. (FTIR, Nicolet ZOSX). Thermo-gravimetric analysis (TGA) curve was recorded using a TGA/SDTA851<sup>e</sup> module from METTLER TOLEDO in nitrogen flow in the temperature range 50–500 °C, the heating rate being 20 °C min<sup>-1</sup> and the data was collected and analyzed with STAR<sup>e</sup> software.

## 3 Results and discussion

As shown in Fig. 1, the fibers which were treated at 200 °C for 1 h still remained amorphous, and when the fibers were held at 300 °C for 1 h, the peaks located at 2 $\theta$  angles of 23, 33, 38, 55 and 66° suggested the occurrence of  $\beta$ -Fe<sub>2</sub>O<sub>3</sub> in addition to the  $\alpha$ -Fe<sub>2</sub>O<sub>3</sub> phase. Upon increasing the heating temperature to 400 °C,  $\beta$ -Fe<sub>2</sub>O<sub>3</sub> completely converted to  $\alpha$ -Fe<sub>2</sub>O<sub>3</sub>. On further

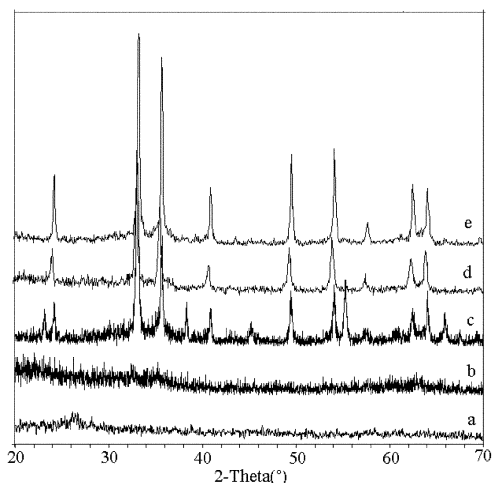


**Fig. 1** XRD patterns of the green gel fibers (a) and the fibers after treatment at 200 °C (b), 300 °C (c), 400 °C (d) and 600 °C (e) for 1 h.

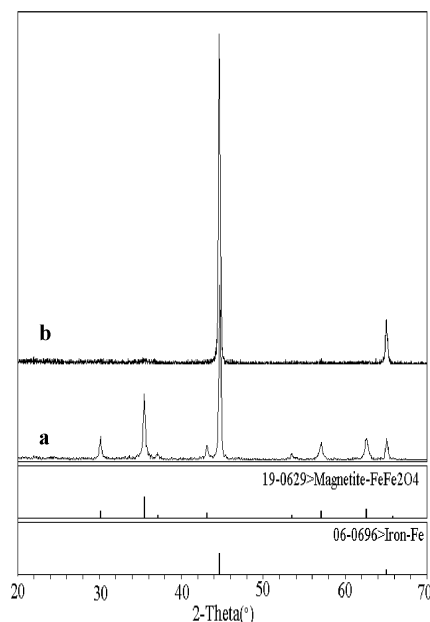
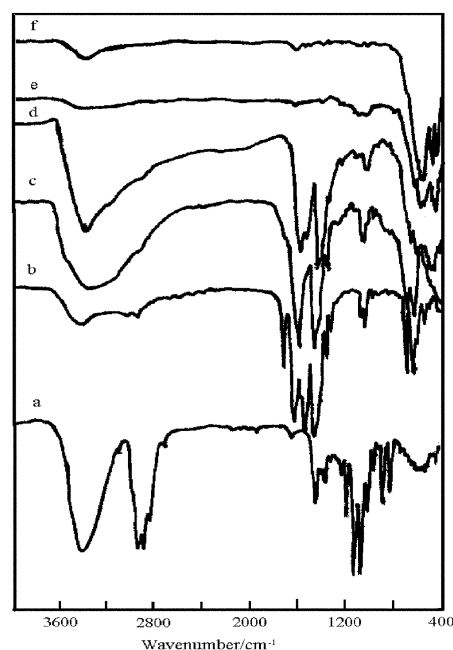


**Fig. 2** The XRD patterns of hollow fibers reduced by hydrogen flow at 350 °C for (a) 0.5 h and (b) 1 h.

increasing the heating temperature, there were no obvious changes in the XRD spectra, only the intensity of the peaks increased and the full width at half-maximum of the hematite Bragg peak decreased, which suggested the growth of the particles.

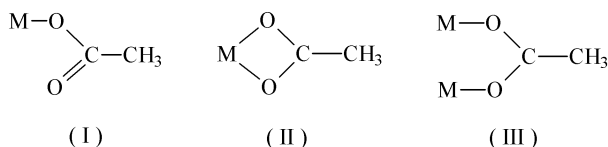
The XRD patterns of the fibers reduced by hydrogen are shown in Fig. 2. It can be seen that when the reaction time was 0.5 h, the product was a mixture of Fe<sub>3</sub>O<sub>4</sub> and  $\alpha$ -Fe. Upon increasing the reaction time to 1 h, phase-pure  $\alpha$ -Fe formed. Obviously, the as-prepared hollow hematite fibers were very easy reduced to  $\alpha$ -Fe, and the reduction condition was mild compared to the bulk counterparts.<sup>13</sup>

Fig. 3 gives the FT-IR spectra of the gel fibers and those heat treated at 200, 300 and 400 °C for 1 h, and the FT-IR spectra of CH<sub>3</sub>OCH<sub>2</sub>CH<sub>2</sub>OH and Fe(OOCCH<sub>3</sub>)<sub>3</sub> are also shown. The IR



**Fig. 3** IR spectra of (a) MOE, (b) ferric acetate, (c) green gel fibers, and of hollow fibers after treatment at (d) 200 °C, (e) 300 °C and (f) 400 °C for 1 h.

spectrum of the carboxylate group demonstrated the characteristic doublet absorption in the wavenumber range 1200–1700  $\text{cm}^{-1}$  due to the asymmetric and symmetric stretching vibrations of  $\text{COO}^-$  ( $\nu_{\text{as}}(\text{OCO})$  and  $\nu_{\text{s}}(\text{OCO})$ ). There are three modes of coordinated carboxylate ligands: monodentate (I), chelating (II) and bridging (III).



The values of  $\nu_{\text{as}}(\text{OCO})$  and the frequency differences between  $\nu_{\text{as}}(\text{OCO})$  and  $\nu_{\text{s}}(\text{OCO})$  offer the most sensitive indication of the mode of carboxylate coordination.<sup>14</sup> Fig. 3b gives a characteristic IR absorption of a metal acetate. The band at 3394  $\text{cm}^{-1}$  is assigned to the stretching vibration of OH, and the bands at 1698 and 1348  $\text{cm}^{-1}$  are ascribed to monodentate  $\nu_{\text{as}}(\text{OCO})$  and  $\nu_{\text{s}}(\text{OCO})$ . There are three bands appearing at 1608, 1519 and 1446  $\text{cm}^{-1}$  and the frequency differences between them are 162 and 73  $\text{cm}^{-1}$ , respectively, suggesting the coexistence of chelating and bridging ligands. The bands between 700–400  $\text{cm}^{-1}$  are ascribed to the stretching vibration of Fe–O. The IR spectrum for gel fibers shown in Fig. 3c is found to have well-defined doublet peaks at 1576 and 1446  $\text{cm}^{-1}$ , and the bands of monodentate and chelating OCO nearly disappear. It can be seen from Fig. 3c that the band assigned to  $\nu_{\text{OH}}$  moves to 3371  $\text{cm}^{-1}$ , which may result from the formation of a hydrogen bond. It can be assumed that the main coordinate mode of the carbonyl oxygen of the acetate to a ferric atom center is bridging giving the chain structure, and hydrogen bonds form, which account for the spinnability of the sol. Fig. 3a gives the typical IR spectrum of MOE. Comparing Fig. 3a and Fig. 3c, it can be concluded that MOE did not bond to iron(III). The FT-IR spectra of the fibers sintered at 200 °C have no obvious changes compared with the spectra of the gel fibers, only the band assigned to  $\nu_{\text{OH}}$  reverted to 3396  $\text{cm}^{-1}$  which may result from the damage of the hydrogen bonds. The IR spectrum of the fiber heated at 300 °C indicates that the organic parts have been removed completely. The peaks at 548 and 472  $\text{cm}^{-1}$  are assigned to  $\alpha\text{-Fe}_2\text{O}_3$  and the bands of  $\beta\text{-Fe}_2\text{O}_3$  are located at 620, 570 and 453  $\text{cm}^{-1}$ . Upon further increasing the heating temperature, the bands of  $\nu(\text{Fe}-\text{O})$  belonging to  $\beta\text{-Fe}_2\text{O}_3$  completely disappear and pure  $\alpha\text{-Fe}_2\text{O}_3$  can be obtained.

Very interestingly, the hollow structure is found after the gel fiber is exposed to air for about one month; even at this stage, there are a large amount of organic moieties remaining in the hollow fiber from the IR spectrum. Fig. 4 shows the SEM images of the gel fibers and the hollow  $\alpha\text{-Fe}_2\text{O}_3$  fibers after calcination at 200 and 400 °C for 1 h. It can be seen from Fig. 4b that the outer diameter of the hollow  $\alpha\text{-Fe}_2\text{O}_3$  fibers is between 4–15  $\mu\text{m}$  with the most frequent ones being around 4–10  $\mu\text{m}$ . Fig. 4c gives the cross-section of the hollow fibers which have been held at 200 °C for 1 h. It clearly indicates that the tube structure forms and the thickness of the wall is between 1–2  $\mu\text{m}$ . The high magnification SEM is used to view the surface particles of the fiber heat treated at 400 °C for 1 h (Fig. 4d). Obviously, the fiber wall is composed of well-defined particles, 100 nm in diameter.

The TEM image of the hollow fiber fired to 400 °C is shown in Fig. 5. A tubular structure can be seen, but it is not obvious because of the non-uniform wall thickness, the visible tube is not located in the middle of the hollow fiber. It is clear that the wall of the fibers is made up of nanoparticles and the particle size is around 100 nm, which agree with the SEM results.

Fig. 6 gives the SEM images of  $\alpha\text{-Fe}$  fibers. It shows that the fiber kept the morphology of the hematite fiber, but the surface

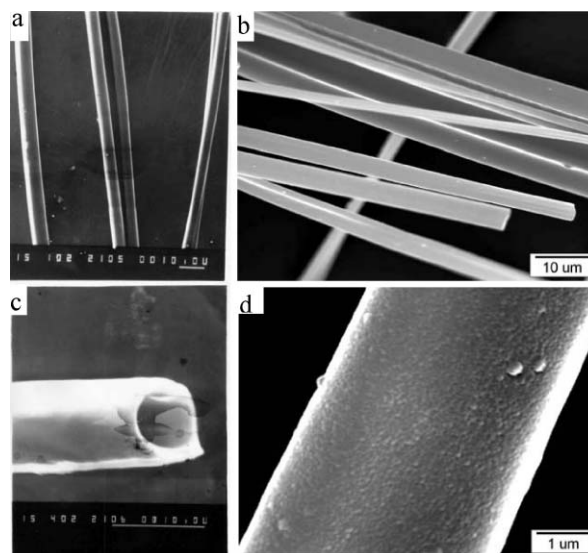


Fig. 4 SEM images of the (a) green gel fibers, (b) fibers after treatment at 400 °C for 1 h, (c) cross-section of a fiber after treatment at 200 °C for 1 h and (d) magnified surface of a fiber after treatment at 400 °C for 1 h.

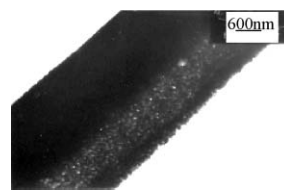


Fig. 5 TEM images of the hollow fibers after treatment at 400 °C for 1 h.

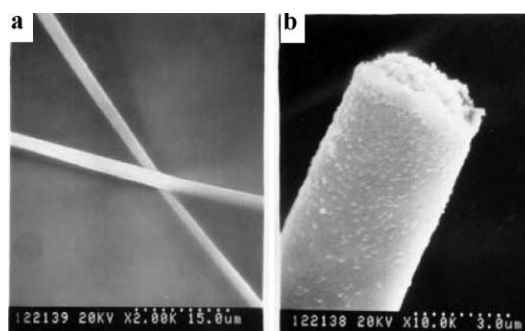


Fig. 6 SEM images of the fibers reduced by hydrogen flow at 350 °C for (a) 0.5 h and (b) 1 h.

particles are as large as 150 nm in diameter. Obviously, the nanoparticles in the fiber become larger after reduction

The effect of the molar ratio ( $n$ ) of  $\text{Fe}(\text{OC}_2\text{H}_5)_3$  to MOE on the property of the sol was studied. It was found that spinnable sol could be obtained when  $n$  changed between 1 : 3 and 1 : 9, but the weight percent solids of the gel fibers were 64% for sample 3 and 48% for sample 5 (Fig. 7), respectively. The thermogravimetric analysis (TGA) curves showed that when the temperature ranged from 140–280 °C, the weight loss of the gel fibers was changed from 19% to 34% when  $n$  changed from 1 : 3 to 1 : 9, but a constant weight loss was held from 280–400 °C. It can be concluded that the former weight loss may be ascribed to the removal of free organic solvent, and the latter one resulted from the decomposition of the acetate groups, which is consistent with the IR results (Fig. 3). Replacing the MOE with other organic compounds such as octanol and 1,2-propanediol or MOE being absent, the spinnable sol could not be obtained. It can be sure that MOE did not bond to iron(III) in the gel fiber from Fig. 3. What is the role of the MOE in the

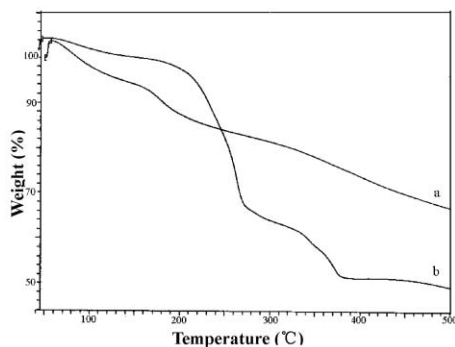
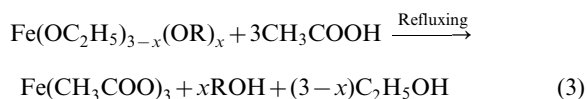
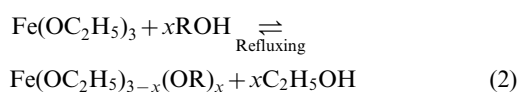


Fig. 7 DTG curves of the gel fibers with the molar ratio of ferric alkoxide to MOE being (a) 1:3 and (b) 1:9.

system? In the present synthesis, the molar ratio of  $\text{Fe}(\text{OC}_2\text{H}_5)_3$  to MOE influences the ageing time (Table 1), and spinnable sols can be obtained while  $n$  is changed from 1:3 to 1:9. Here, the possible formation mechanism of the spinnable sol is as follows. The  $-\text{OC}_2\text{H}_5$  of the  $\text{Fe}(\text{OC}_2\text{H}_5)_3$  molecule can be replaced by an alkoxy group ( $-\text{OR}$ ) from the other alcohol, which is termed an alcohol-interchanging reaction (eqn. (2)).<sup>12</sup> The formed ferric alkoxide ( $\text{Fe}(\text{OC}_2\text{H}_5)_{3-x}(\text{OR})_x$ ) could react with acetic acid through a bridging mode to form  $\text{Fe}(\text{CH}_3\text{COO})_3$  (eqn. (3)) and  $\text{Fe}(\text{CH}_3\text{COO})_3$  further polymerized to give the chain structure. However, unlike 1,2-propanediol or octanol, the MOE molecule can hydrogen-bond to the  $\text{Fe}(\text{CH}_3\text{COO})_3$  chain polymer to produce a spinnable sol, and the formed  $\text{Fe}(\text{CH}_3\text{COO})_3$  in 1,2-propanediol and octanol solvents is actually a colloidal deposition due to the self-polymerization of  $\text{Fe}(\text{CH}_3\text{COO})_3$  chains. During the formation of the spinnable sol, absolute ethanol worked as solvent.



The possible process for the formation of the hollow structure is described as follows. When the green fiber was drawn out, a rigid outer shell was formed, but the interior of the drawing fiber was still fluid at this stage,<sup>4</sup> and a large amount of alcohol and acetate anions remained in the gel fibers. When the gel fiber was fired in a tubular furnace, the sol particles diffused to the inner surface of the outer shell with the evaporation of the organic compounds, and thus the tube first formed. Even at this stage, there were still many organic parts remaining in the fibers, which can be seen from IR results. Upon increasing the heating temperature, acetate anions began to decompose to produce  $\text{CO}_2$  and  $\text{H}_2\text{O}$  gases, which went out of the fibers through the tube, and a crystallized hollow fiber produced.

## 4 Conclusion

Continuous hollow  $\alpha\text{-Fe}_2\text{O}_3$  fibers have been prepared by a sol-gel method using ferric alkoxide containing acetic acid as starting materials. The outer diameter of the as-prepared hollow fibers is 4–20  $\mu\text{m}$  with most frequent ones being 4–10  $\mu\text{m}$  and the wall thickness is between 1–2  $\mu\text{m}$ . Hollow  $\alpha\text{-Fe}$  fibers are also prepared by reducing the as-prepared  $\alpha\text{-Fe}_2\text{O}_3$  fibers under hydrogen flow at 350  $^\circ\text{C}$  for only 1 h. The possible mechanism for the formation of the continuous hollow fiber is given as follows. Ferric acetate formed with the main coordination mode of the acetate anion to ferric being bridging and MOE hydrogen-bonded to ferric acetate, which resulted in the spinnable sol. A dense outer shell came into being as soon as the gel fiber was drawn. A tube structure first formed with the organic compounds vaporizing, and the tube structure was kept in the decomposed process of acetate anions.

The hollow ferric-based fibers have potential applications in catalytic and materials science. Currently, detailed studies are in progress to modify the hollow fibers with nano-materials to organize micro-nano devices.

## References

- 1 C. G. Wu and T. Bein, *Science*, 1994, **264**, 1757; C. G. Wu and T. Bein, *Science*, 1994, **266**, 1013; S. A. Johnson, E. S. Brigham, P. T. Ollivier and T. E. Mallouk, *Chem. Mater.*, 1997, **9**, 2448; S. A. Johnson, D. Khushalani, N. Coombs, T. E. Mallouk and G. A. Ozin, *J. Mater. Chem.*, 1998, **8**, 13; J. Lee, S. Yoon, S. M. Oh, C. H. Shin and T. Hyeon, *Adv. Mater.*, 2000, **12**, 359; J. Jang, B. Lim, J. Lee and T. Hyeon, *Chem. Commun.*, 2001, 83.
- 2 H. Kozuka, T. Umeda, J. S. Jin and S. Sakka, Paper Presented at Materials Research Society, Spring Meeting, Reno, 1988; S. Sakka, H. Kozuka and T. Umeda, *J. Ceram. Soc. Jpn.*, 1988, **96**, 468.
- 3 H. Zhuang, H. Kozuka and S. Sakka, *Jpn. J. Appl. Phys.*, 1989, **28**(10), L1805.
- 4 M. Aizawa, Y. Nakagawa, Y. Nosaka, N. Fujii and H. Miyama, *J. Non-Cryst. Solids*, 1990, **124**, 112.
- 5 S. Kobayashi, K. Hanabusa, N. Hamasaki, M. Kimura and H. Shirai, *Chem. Mater.*, 2000, **12**, 1523.
- 6 H. Nakamura and Y. Matsui, *J. Am. Chem. Soc.*, 1995, **117**, 2651.
- 7 Y. Ono, Y. Kanekiyo, K. Inoue, J. Hojo, M. Nango and S. Shinkai, *Chem. Lett.*, 1999, 475; Y. Ono, K. Nakashima, M. Sano, J. Hojo and S. Shinkai, *Chem. Lett.*, 1999, 1119; Y. Ono, K. Nakashima, M. Sano, J. Hojo and S. Shinkai, *J. Mater. Chem.*, 2001, **11**, 2412.
- 8 J. Kiwi and M. Crätzel, *J. Chem. Soc., Faraday Trans. 1*, 1987, **83**, 1101; B. C. Faust, M. R. Hoffmann and D. W. Bachmann, *J. Phys. Chem.*, 1989, **93**, 6371.
- 9 K. Široký, J. Jirešová and L. Hudec, *Thin Solid Films*, 1994, **245**, 211; G. Neri, A. Bonavita, S. Galvagno, P. Siciliano and S. Capone, *Sens. Actuators, B: Chem.*, 2002, **82**(1), 40.
- 10 C. E. Boyer, E. J. Borchers, R. J. Kuo and C. D. Hoyle, *US Pat.* 5085931, 1992.
- 11 M. Adachi, Y. Murata, M. Harada and S. Yoshikawa, *Chem. Lett.*, 2000, 942.
- 12 D. C. Bradley, R. C. Mehrotra and D. P. Guar, *Metal Alkoxide*, Academic Press, London, 1978.
- 13 A. E. Regazzoni, G. A. Urrutia, M. A. Blesa and A. J. G. Maroto, *J. Inorg. Nucl. Chem.*, 1981, **43**, 1489.
- 14 S. D. Robinson and M. F. Uttley, *J. Chem. Soc., Dalton Trans.*, 1973, 1912.